Clin Pharmacokinet (2015) 54:305–317
DOI 10.1007/s40262-014-0212-8

ORIGINAL RESEARCH ARTICLE

A Population Pharmacokinetic Model of Valproic Acid in Pediatric Patients with Epilepsy: A Non-Linear Pharmacokinetic Model Based on Protein-Binding Saturation

Junjie Ding · Yi Wang · Weiwei Lin · Changlian Wang · Limei Zhao · Xingang Li · Zhigang Zhao · Liyan Miao · Zheng Jiao

Published online: 12 November 2014

Abstract

Background and Objective Valproic acid (VPA) follows a non-linear pharmacokinetic profile in terms of protein-binding saturation. The total daily dose regarding VPA clearance is a simple power function, which may partially explain the non-linearity of the pharmacokinetic profile; however, it may be confounded by the therapeutic drug monitoring effect. The aim of this study was to develop a population pharmacokinetic model for VPA based on protein-binding saturation in pediatric patients with epilepsy.

Methods A total of 1,107 VPA serum trough concentrations at steady state were collected from 902 epileptic pediatric patients aged from 3 weeks to 14 years at three hospitals. The population pharmacokinetic model was developed using NONMEM® software. The ability of three candidate models (the simple power exponent model, the dose-dependent maximum effect [DDE] model, and the protein-binding model) to describe the non-linear pharmacokinetic profile of VPA was investigated, and potential covariates were screened using a stepwise approach. Bootstrap, normalized prediction distribution errors and external evaluations from two independent studies were performed to determine the stability and predictive performance of the candidate models.

Results The age-dependent exponent model described the effects of body weight and age on the clearance well. Co-medication with carbamazepine was identified as a significant covariate. The DDE model best fitted the aim of this study, although there were no obvious differences in the predictive performances. The condition number was less than 500, and the precision of the parameter estimates was less than 30 %, indicating stability and validity of the final model.

Conclusion The DDE model successfully described the non-linear pharmacokinetics of VPA. Furthermore, the proposed population pharmacokinetic model of VPA can be used to design rational dosage regimens to achieve desirable serum concentrations.

J. Ding and Y. Wang contributed equally to this study.

J. Ding · Y. Wang
Children's Hospital, Fudan University, Shanghai, China

W. Lin · C. Wang
Department of Pharmacy, The First Hospital Affiliated to Fujian Medical University, Fuzhou, China

L. Zhao
Department of Pharmacy, Shengjing Hospital of China Medical University, Shenyang, China

X. Li · Z. Zhao
Department of Pharmacy, Beijing Tian Tan Hospital, Capital Medical University, Beijing, China

L. Miao
Department of Pharmacy, The First Hospital affiliated to Soochow University, Soochow, China

Z. Jiao (✉)
Department of Pharmacy, Huashan Hospital, Fudan University, 12 Wu Lu Mu Qi M Rd, Shanghai 200040, China
e-mail: zjiao@fudan.edu.cn

Key Points

This study represents the largest population pharmacokinetic study of valproic acid (VPA) conducted to date in pediatric patients ($n = 902$) and covers a wide age range of 3 weeks to 14 years.

A new population pharmacokinetic model was proposed to describe the non-linear pharmacokinetic profile of VPA in terms of protein-binding saturation.

The established model was comprehensively evaluated and shown to have stability and validity, and this model could be used for the design of rational dosage regimens for pediatric patients with epilepsy.

1 Introduction

Epilepsy is one of most common chronic neurological disorders in childhood and is characterized by recurrent seizures. The reported prevalence of epilepsy in children ranges from 4 to 9 per 1,000 children worldwide [1]. Epilepsy is most commonly treated with anti-epileptic drugs (AEDs), and valproic acid (VPA) is a frequently prescribed AED for children [2, 3] due to its broad spectrum of activity against both partial and generalized seizures [4, 5].

There are at least three routes of VPA metabolism in humans: glucuronidation and beta oxidation in the mitochondria, which account for 50 and 40 % of the dose, respectively, as well as cytochrome P450-mediated oxidation and hydroxylation, which account for approximately 10 % of the dose [6–8]. This drug has a low hepatic extraction ratio and a high plasma protein-binding ratio (90–95 %) [9, 10]. VPA exhibits saturable binding to plasma proteins, which results in a higher unbound fraction at high serum concentrations. The concentration-dependent protein binding of VPA causes the drug to follow non-linear pharmacokinetics [11].

VPA has wide inter- and intra-individual pharmacokinetic variability, and its narrow therapeutic range (50–100 mg/L) necessitates close monitoring and individualized dosing regimens [12]. Insight into the sources of the large pharmacokinetic variability in VPA and a dosing method that considers the factors that affect this variability is desirable. Several studies have described the population pharmacokinetic characteristics of VPA in children with epilepsy and have suggested that age, body weight (BW), and co-therapy with enzyme-inducing AEDs have definite impacts on the pharmacokinetics of VPA [13–19]. However, the inclusion of dose in the VPA population pharmacokinetic model to interpret the non-linear pharmacokinetic profile remains controversial. Three previous studies did not include dose as a covariate in the model [17–19], but four other studies did include the dose in VPA clearance as a simple power function, which might partially explain the non-linearity of the pharmacokinetic profile in terms of protein-binding saturation [13–16]. Any of these models may be strongly confounded by the therapeutic drug monitoring (TDM) effect, which can be misinterpreted as non-linearity in the pharmacokinetic model [20]. In the clinical setting, patients with higher clearance will have a lower concentration of the drug and will be administered higher doses, and vice versa. Correlation between dose and clearance is induced during the TDM process and could lead to the interpretation that clearance is a non-linear function of dose, even when non-linearities do not exist; this effect is defined as the TDM effect.

The aim of this study is to develop a population pharmacokinetic model for VPA based on protein-binding saturation in pediatric epileptic patients using routine TDM data obtained from multicenter studies.

2 Methods

2.1 Patients

Data from 902 epileptic children, including 1,107 measured serum VPA concentrations that were obtained during routine clinical visits, were collected from three hospitals and were used to construct the model [16, 21]. VPA was administered orally one to four times a day in the form of a syrup (Depakine®, Hangzhou Sanofi Minsheng Pharmaceutical Co. Ltd., Hangzhou, China), conventional tablets (Baoqing®, Hunan Xiangzhong Pharmaceutical Co., Hunan, China), or sustained release (SR) tablets (Depakine®, Hangzhou Sanofi Minsheng Pharmaceutical Co. Ltd.). After at least 1 week of VPA administration, the patients were assumed to have reached steady-state serum concentrations, and blood samples were collected shortly before the next dose.

Compliant patients with at least one VPA trough concentration and complete records of BW, age, sex, co-therapy with other AEDs, dosing history, and sampling time were included in the current analysis. Those who had renal or hepatic impairment or abnormal albumin level laboratory results (normal range: 3.5–5.0 g/dL) were excluded. Patients administered other drugs that may have affected the pharmacokinetics of VPA (traditional Chinese medicines, aspirin, and carbapenems, including meropenem and imipenem) were excluded from the study. The

study protocols were approved by the independent ethics committee of each study hospital.

2.2 Bioassay

The serum VPA concentration was measured using fluorescence polarization immunoassay (TDx or TDxFlx®, Abbott Laboratories, Abbott Park, IL, USA) in each study center using a calibration range of 12.5–150 mg/L. The inter- and intra-coefficients of variation for this assay were less than 10 %.

2.3 Population Pharmacokinetic Model Development

Population pharmacokinetic analysis was performed using the NONMEM® program (version 7.2, ICON Development Solutions, Ellicott City, MD, USA), which was compiled using gFortran (version 4.60). R (version 14.2, http://www.r-project.org/) was used to construct the output visualizations and the model evaluations. The first-order conditional estimation method including η–ε interaction (FOCE-I) was used throughout the model-building procedure.

2.3.1 Base Model

Based on previous reports, the time course of VPA concentrations was modeled using a one-compartment model with first-order absorption and first-order elimination; the model was parameterized in terms of apparent total clearance (CL/F), absorption rate constant (k_a), and apparent volume of distribution (V_d/F). Due to a lack of information regarding the absorption phase, the k_a was fixed at values of 2.64, 1.57, and 0.46 h^{-1} for syrup, conventional tablets, and SR tablets, respectively [22, 23]. VPA was administered orally one to four times, and the time after the last dose (TAD) covered a wide range from 6.0 to 27.5 h, with a median TAD of 12.2 h (Fig. 1). Therefore, V_d/F was modeled using Eq. 1, as suggested previously [24, 25]:

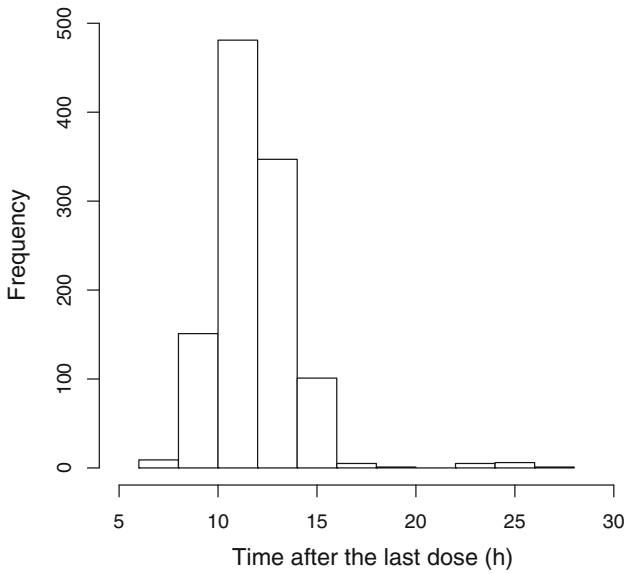

Fig. 1 Histogram of the distribution of time after the last dose

$$V_d/F = V_p \cdot \left(\frac{BW}{70}\right) \quad (1)$$

where V_p is the typical value of V_d/F scaled to a 70-kg adult.

Exponential models were used to account for inter-subject variability (ISV). The value of a parameter for an individual (P_i) is a function of the parameter value ($\widehat{P}$) for a typical individual and an individual deviation represented by η_i. η_i is defined as a symmetrically distributed, zero-mean random variable with a variance that is estimated as part of the model estimation from Eq. 2:

$$P_i = \widehat{P} \times \exp(\eta_i) \quad (2)$$

The following statistical models describing the random residual variability (RUV) were considered (Eqs. 3–5):

$$Y = \text{IPRED} + \varepsilon \quad (3)$$

$$Y = \text{IPRED} \times \exp(\varepsilon) \quad (4)$$

$$Y = \text{IPRED} \times \exp(\varepsilon_1) + \varepsilon_2 \quad (5)$$

where Y represents the observation, IPRED is the individual prediction, and ε_n represents the symmetrically distributed zero-mean random variables with variance terms that are estimated as part of the population model-fitting process. The effects of the three different studies were considered by adding these effects to the RUV model.

2.3.2 Covariate Models

The investigated covariates included sex, BW, age, formulation (syrup, conventional tablet, or SR tablet), and co-therapy with other AEDs (more than 10 % of total patients). Because only trough data were collected, the covariates were investigated only for the CL/F.

It is well-known that age and/or BW have significant impacts on the CL/F of VPA in pediatric patients [14–16, 18, 19, 25–29]. Therefore, age and BW were included in the model first. Because BW was proven to be superior over age as a covariate for clearance, six different models based on BW scaling of the intrinsic clearance were tested using Eq. 6 [24]. The models exhibiting the best fits were selected for further analysis.

$$CL/F = CL_P \cdot \left(\frac{BW}{70}\right)^{k_1} \cdot F_{mat} \quad (6)$$

where CL_p is the clearance in a 70-kg adult and F_{mat} represents the fraction of the adult value of clearance and it was fixed to 1, except when using model III.

Model I: The 3/4 allometric model [24]; the exponent k_1 was fixed to 0.75.

Model II: The simple exponent model; the exponent k_1 was estimated.

Model III: The maturation model [24]; the exponent k_1 was fixed to 0.75, and F_{mat} was calculated according to Eq. 7.

$$F_{mat} = \frac{1}{1 + \left(\frac{Age}{TM_{50}}\right)^{-\gamma}} \quad (7)$$

where TM_{50} is the value of age when maturation reaches 50 % of the adult clearance, and γ is the Hill coefficient used to determine the steepness of the sigmoid decline.

Model IV: The age-cutoff separated model; different values for the exponent k_1 were estimated in model II for two sub-populations according to the age-cutoff.

Model V: The BW-dependent exponent (BDE) model [29] (Eq. 8).

$$k_1 = k_0 - \frac{k_{max} \cdot BW^{\gamma}}{k_{50}^{\gamma} + BW^{\gamma}} \quad (8)$$

Model VI: The age-dependent exponent (ADE) model (Eq. 9).

$$k_1 = k_0 - \frac{k_{max} \cdot Age^{\gamma}}{k_{50}^{\gamma} + Age^{\gamma}} \quad (9)$$

where k_0 is the value of the exponent at a theoretical BW of zero (model V) or at birth (0 years) (model VI), k_{max} is the maximum decrease of the exponent, k_{50} is the BW (model V) or age (model VI) at which a 50 % decrease in the maximum decrease is attained, and γ is the Hill coefficient used to determine the steepness of the sigmoid decline.

At the second step, the covariate of carbamazepine was included proportionally to CL/*F* in the model because carbamazepine is an enzyme-inducing drug and can increase the CL/*F* of VPA [16–18, 21]. The remaining potential covariates (sex, formulation, and co-medication with other AEDs) were then tested sequentially by forward inclusion and backward elimination approaches using proportional equations.

Third, the following three models, which describe the non-linear pharmacokinetic characteristics of VPA, were tested:

Model VII: The simple exponent model (Eq. 10).

$$CL/F = CL_p \cdot \left(\frac{TDD}{25}\right)^{k} \quad (10)$$

where TDD represents total daily dose (mg/kg).

Model VIII: The dose-dependent maximum effect (E_{max}) model (DDE) was used to describe the relative change of clearance (CL/*F*) due to the increasing unbound fraction of drug that occurs as the dose increases (Eq. 11).

$$CL/F = CL_p \cdot \left(1 + \frac{E_{max} \cdot TDD^{\gamma}}{TDD_{50}^{\gamma} + TDD^{\gamma}}\right) \quad (11)$$

where TDD_{50} represents the TDD when E_{max} is increased by 50 %.

The 2.5th and 97.5th percentiles of the observed total VPA concentrations in the current study were 25 and 121 mg/L, and the corresponding fraction unbound (f_u) values were 5 and 19 %, respectively, according to a previous report [30]. When TDD $\gg$ TDD_{50}, E_{max} was 2.8 as shown in Eq. 12:

$$1 + \frac{E_{max} \cdot TDD^{\gamma}}{TDD_{50}^{\gamma} + TDD^{\gamma}} \approx 1 + E_{max} = \frac{19\%}{5\%} = 3.8 \quad (12)$$

where $(1 + E_{max})$ represented the maximum relative change of the f_u.

Model IX: The protein-binding model was employed to describe the non-linear pharmacokinetics in terms of protein-binding saturation [31–33] (Eqs. 13 and 14).

$$C_b = \frac{B_m \times C_f}{K_d + C_f} \quad (13)$$

$$C_t = C_b + C_f \quad (14)$$

where C_b and C_f are the bound and unbound serum concentrations of VPA, respectively. B_m (mg/L) is the apparent maximum concentration of the binding site for VPA, and K_d (mg/L) is the apparent dissociation constant of VPA. Because the unbound serum concentration of VPA were not measured in our study, the values of B_m and K_d used in Eq. 13 were fixed to 130 and 7.8 mg/L, respectively, for patients over 1 year of age and to 114 and 7.0 mg/L, respectively, by standardizing to a 7.5 kg patient in those aged under 1 year; these values were obtained from previously published studies of Japanese pediatric epilepsy patients [31, 32].

2.3.3 Covariate and Model Selection Criteria

Because fewer numbers of observations per subject in our study may be associated with a higher amount of shrinkage [34], nested models were statistically compared using a likelihood ratio test on the differences in the objective function value (OFV). Statistical significance was set at $p < 0.001$. Akaike information criteria (AIC) and Bayesian information criteria (BIC) calculated using Pirana software (version 2.7.1, Pirana Software & Consulting BV, http://www.pirana-software.com/) were used to select competing, non-nested models [35]. Models with lower AICs and BICs were considered superior [36].

Clinical significance and biological plausibility of covariate addition was also considered, and a 20 % change was chosen as the cutoff for clinical significance [37–39]. Scatterplots of the conditional weighted residuals, standard

errors of the parameter estimates, and changes in the estimates of ISV and RUV were also examined.

In addition, two datasets obtained from independent studies were used to select the non-linear pharmacokinetic model; these data included data for 50 pediatric epileptic patients with 147 VPA trough measurements obtained from Beijing Tian Tan Hospital (Beijing, China), and data for 82 epileptic children with 137 VPA trough concentrations obtained from Shenyang Shengjing Hospital (Shenyang, China) [40]. Population predictions (PREDs) estimated using candidate models were compared to the observations (OBS) using the MAXEVAL = 0 option. Mean prediction error (MPE) and mean absolute prediction error (MAE) were calculated to determine the bias and imprecision of the predictive performance [41] (Eqs. 15 and 16). In addition, the number of patients with MPE beyond ±20 and ±30 % were calculated. The models with lowest MPE and MAE values and the fewest number of prediction errors beyond ±20 and ±30 % were considered superior.

$$\mathrm{MPE}\% = \frac{1}{N}\sum \frac{\mathrm{PRED}_i - \mathrm{OBS}_i}{\mathrm{OBS}_i} \times 100\% \quad (15)$$

$$\mathrm{MAE}\% = \frac{1}{N}\sum \left|\frac{\mathrm{PRED}_i - \mathrm{OBS}_i}{\mathrm{OBS}_i}\right| \times 100\% \quad (16)$$

2.4 Model Evaluation

In addition to the approach described above, bootstrap [42] and normalized prediction distribution errors (NPDEs) [43] were employed to evaluate the model. Using the Perl-speaks-NONMEM program (PsN, version 3.5.3, http://psn.sourceforge.net) 2,000 bootstrap datasets were generated. The final population pharmacokinetic model was fitted to each of these bootstrap datasets, and all model parameters were estimated. The median and the 2.5th–97.5th percentile intervals were calculated and compared with the values obtained using NONMEM®.

Simulation of NPDE was performed 2,000 times, and each observation was compared to the simulated reference distribution. A histogram of the NPDE distribution and plots of NPDE versus PRED and versus TAD were used to evaluate the final model. The NPDE evaluation was performed using an add-on package in R [43].

2.5 Simulation of Dosing Regimen

The final proposed model could be used to estimate the dosage for a given pediatric patient who achieved the target VPA concentration of 50–100 mg/L, which might facilitate an optimal dosage regimen. In addition, covariates were constructed for typical pediatric patients aged 6 months and above based on the China National Survey of Body Weight for children [44].

3 Results

3.1 Patient Demographic Data

A summary of the demographic characteristics of the patients used for model development and evaluation is given in Table 1. Age, BW, and sex did not significantly differ between the model development dataset and model evaluation datasets.

3.2 Population Pharmacokinetic Model Development

Based on the OFV and the distribution of residuals in the diagnostic plots of the base model, an additive error model was selected to model the RUV. In addition, the change of OFV was not significant if separate RUV terms for three centers were used in the model. The ISV of the V_d/F was very small ($<1 \times 10^{-4}$) and was removed from the model. The base model had an OFV of 8,669.4, with η- and ε-shrinkage of 29.8 and 22.8 %, respectively.

To account for BW and age, six various allometric equations for clearance were evaluated (Table 2). Among the six models examined, the ADE model (Model VI) had the lowest AIC (8,229.2) and BIC (8,269.2) and was employed in further analyses.

Co-medications included carbamazepine, topiramate, clonazepam, phenobarbital, lamotrigine, levetiracetam, oxcarbazepine, and phenytoin. The first three co-medications were taken by more than 10 % of all study patients and were considered in the further covariate screening. The inclusion of carbamazepine decreased the OFV by 183.5 ($p < 0.001$) and increased the CL/F by 50 %. Incorporating topiramate did not affect the CL/F, but including clonazepam increased the CL/F by 16 % (ΔOFV = 32.7, $p < 0.001$). Moreover, the CL/F of females was 7 % higher than that of males (ΔOFV = 12.6, $p < 0.001$), and the administration of SR tablets decreased the CL/F by 17 % (ΔOFV = 22.3, $p < 0.001$). However, all of the observed changes except co-medication with carbamazepine were less than 20 %, which might have no clinical significance and were not retained in the model.

Then, three candidate models (model VII–IX) describing the non-linear VPA pharmacokinetic were compared, and this comparison showed that the DDE model (model VIII) had lower AIC and BIC values than those of the simple exponent model (model VII) and protein-binding model (model IX) (AIC: 7,772.3 vs. 7,772.6 and 7,792.2; BIC: 7,822.4 vs. 7,822.6 and 7,837.3, respectively). The condition numbers for all candidate models were less than 500, and the standard error of parameter estimates were less than 30 %, which demonstrated the stability of the proposed models [36].

Table 1 Demographic data of pediatric epilepsy patients

Characteristic	Model development sets				Model external evaluation sets	
	Children's Hospital of Fudan University	Huashan Hospital of Fudan University	The First Affiliated Hospital of Fujian Medical University	Total	Beijing Tian Tan Hospital	Shenyang Shengjing Hospital
No. of patients/VPA samplings	307/366	176/207	419/534	902/1,107	50/147	82/137
Male/female, *n*	187/120	100/76	260/159	547/355	35/15	49/33
Age (years)	1.8 (3 weeks–13.8) [3.3 ± 3.5]	9.0 (0.3–14.0) [8.7 ± 3.2]	5.8 (0.5–14.0) [6.0 ± 3.2]	5.3 (3 weeks–14.0) [5.7 ± 3.8]	5.8 (4 weeks–13.8) [5.9 ± 3.8]	6.0 (0.25–14.0) [6.2 ± 4.5]
Body weight (kg)	11.0 (2.6–70.0) [14.5 ± 10.1]	28.5 (7.5–65.0) [30.0 ± 11.2]	20.0 (7.5–70.0) [23.0 ± 10.7]	19.0 (2.6–70.0) [21.6 ± 11.9]	19.0 (4.9–35.5) [19.2 ± 7.8]	22.0 (5.5–62.0) [25.7 ± 15.1]
VPA daily dose (mg/kg)	30.2 (9.1–60) [30.6 ± 8.4]	22.7 (5.1–54.2) [24.2 ± 9.4]	25.1 (6.5–63.2) [25.7 ± 8.9]	26.7 (5.1–63.2) [27.1 ± 9.2]	12.6 (6.5–97.9) [25.4 ± 14.9]	16.8 (6.8–64.3) [19.0 ± 9.5]
Sampling time after the last dose (h)	11.8 (8.0–23.8) [11.2 ± 1.4]	12.5 (6.3–25.5) [12.6 ± 2.3]	12.7 (6.0–27.5) [12.8 ± 2.0]	12.2 (6.0–27.5) [11.8 ± 2.0]	13.0 (5.0–14.0) [12.3 ± 2.6]	13.0 (5.0–22.2) [13.4 ± 2.3]
VPA concentration (mg/L)	59.9 (16.8–140.9) [62.2 ± 24.2]	81.0 (22.6–149.4) [81.3 ± 29.4]	65.0 (15.0–133.0) [65.7 ± 20.2]	66.0 (15.0–149.4) [67.5 ± 24.5]	75.1(25.4–144.9) [73.8 ± 22.7]	65.9 (12.0–128.8) [66.4 ± 24.9]
No. of patients (%) co-medicated with other antiepileptic drugs						
Total[a]	157 (51.1)	47 (26.7)	107 (25.5)	311 (34.5)	8 (16.0)	17 (20.7)
Carbamazepine	15 (4.9)	43 (24.4)	45 (10.7)	103 (11.4)	3 (6.0)	17 (20.7)
Clonazepam	121 (39.4)	9 (5.1)	14 (3.3)	144 (16.0)	0	0
Lamotrigine	7 (2.3)	0	5 (1.2)	12 (1.2)	0	2 (2.4)
Levetiracetam	13 (4.2)	0	49 (11.7)	62 (6.9)	0	0
Oxcarbazepine	1 (0.3)	0	5 (1.2)	6 (0.6)	0	0
Phenobarbital	11 (3.6)	3 (1.7)	5 (1.2)	19 (2.1)	0	0
Phenytoin	0	0	1 (0.2)	1 (0.1)	0	0
Topiramate	55 (17.9)	1 (0.6)	39 (9.3)	95 (10.5)	6 (12.0)	0

Data are expressed as median (range) [mean ± standard deviation] unless specified otherwise

VPA valproic acid

[a] The number of patients co-medicated with at least one other antiepileptic drug were summarized

Moreover, the predictive performance of these three models was evaluated using two external datasets, and the results are presented in Table 3. Based on the above-mentioned assessments, the DDE model best fitted the aim of the study and was expressed using Eqs. 17 and 18:

$$\mathrm{CL}/F = 0.300 \cdot 1.43^{\mathrm{CBZ}} \cdot \left(\frac{\mathrm{BW}}{70}\right)^{0.791-\frac{0.096\cdot \mathrm{Age}^{8.63}}{0.802^{8.63}+\mathrm{Age}^{8.63}}} \cdot \left(1+\frac{2.8\cdot \mathrm{TDD}^{1.68}}{37.4^{1.68}+\mathrm{TDD}^{1.68}}\right) \quad (17)$$

$$V_{\mathrm{d}}/F = 22.2 \cdot \left(\frac{\mathrm{BW}}{70}\right) \quad (18)$$

where CBZ is carbamazepine and CBZ = 1 for patients co-medicated with carbamazepine, otherwise CBZ = 0. The η- and ε-shrinkage values were 21.8 and 29.5 %, respectively, in the final model.

The typical values for the CL/F of VPA in a 20-kg child (5 years of age, TDD of 30 mg/kg, monotherapy) obtained in our study was 0.27 L/h, which was consistent with the previously reported values of approximately 0.29 L/h [18, 19]. The V_{d}/F was 0.31 L/kg, which was also consistent with a previous report (0.1–0.4 L/kg) [11]. BW with age, co-medicated with carbamazepine, and TDD reduced the ISV of CL/*F* by 15.7, 16.9, and 21.7 %, respectively.

3.3 Model Evaluation

The goodness-of-fit plots for the base and final proposed models are presented in Fig 2. Compared to the base model, the final model was greatly improved, although the low OBS was slightly under-predicted and the high OBS was slightly over-predicted.

In a 2,000-run bootstrap analysis, 74 runs (3.7 %) were terminated due to rounding errors and were excluded from the analysis. A summary of the bootstrap procedure is presented in Table 4. No difference greater than 5 % compared with the corresponding NONMEM® results was observed in the parameter estimates. The symmetric 95 %

Table 2 Parameter estimates of the six bodyweight-dependent clearance candidate models

Parameters	Model I 3/4 Allometric model	Model II Allometric model	Model III 3/4 Allometric and age maturation function model	Model IV Age-cutoff model	Model V BW-dependent exponent model	Model VI Age-dependent exponent model
Model description	$CL_p \cdot (BW/70)^{0.75}$	$CL_p\ (BW/70)^{k_1}$	$CL_p\ (BW/70)^{0.75} \cdot F_{mat}$	$CL_p\ (BW/70)^{k_1}$	$CL_p\ (BW/70)^{k_1}$	$CL_p\ (BW/70)^{k_1}$
Objective function value	8,300.5	8,286.5	8,301.0	8,228.7	8,235.6	8,213.2
Akaike information criteria	8,308.5	8,296.5	8,313.0	8,242.7	8,251.6	8,229.2
Bayesian information criteria	8,328.5	8,321.5	8,343.0	8,277.8	8,291.6	8,269.2
CL_p (L/h)	0.572 (3.0)	0.552 (4.1)	0.572 (2.6)	0.492 (3.2)[a]/0.699 (20.5)[b]	0.478 (4.1)	0.466 (4.1)
k_1	–	0.667 (4.7)	–	0.515 (5.4)[a]/0.807 (11.1)[b]	–	–
$F_{mat} = 1/[1 + (age/TM_{50})^{-\gamma}]$	–	–	1.0[c]	–	–	–
$k_1 = k_0 - k_{max} \cdot BW^{\gamma}/(k_{50}{}^{\gamma} + BW^{\gamma})$ or $k_1 = k_0 - k_{max} \cdot age^{\gamma}/(k_{50}{}^{\gamma} + age^{\gamma})$						
k_0	–	–	–	–	0.671 (3.8)	0.697 (5.4)
k_{max}	–	–	–	–	0.185 (20.8)	0.254 (24.0)
k_{50} (years or kg)	–	–	–	–	9.22 (6.9)	0.858 (28.1)
γ	–	–	–	–	7.34 (48.6)	1.61 (41.6)
$V_p \cdot (BW/70)$ (L/70 kg)	12.5 (9.0)	16.7 (24.8)	12.5 (8.9)	20.5 (10.5)	20.2 (10.4)	20.7 (10.3)
$\omega_{CL/F}$	0.255 (7.0)	0.268 (12.9)	0.255 (7.2)	0.265 (7.5)	0.267 (7.6)	0.265 (7.5)
η-shrinkage (%)	15.0	15.2	15.0	16.4	16.0	16.1
σ (additive mg/L)	14.8 (8.0)	14.8 (12.6)	14.8 (7.9)	14.9 (7.9)	14.7 (7.9)	14.6 (7.9)
ε-shrinkage (%)	36.0	35.8	36.0	34.5	35.0	34.8

Estimates are expressed as estimate (% standard error)

γ Hill coefficient determining the steepness of the sigmoidal decline, *BW* body weight, CL_p typical value of apparent clearance, F_{mat} the fraction of the adult value of clearance, k_0 value of the exponent at a theoretical BW of 0 kg or age at birth, k_1 exponent coefficient of BW, k_{50} the BW or age at which there is a 50 % decrease in the k_{max}, k_{max} maximum decrease, TM_{50} the value of age when 50 % of the adult clearance is attained through maturation, V_p typical value of apparent volume of distribution, $\omega_{CL/F}$ inter-subject variability of apparent clearence, σ residual variability

[a] Estimates for children ≤1 year of age

[b] Estimates for children >1 year of age

[c] The estimated Hill coefficient was 0.02, and then the F_{mat} was equal to 1

confidence intervals were also consistent with the 2.5th–97.5th percentile bootstrap estimates.

In the NPDE analysis, no trend in the scatterplots was observed (Fig.3). The *p* values obtained using the Wilcoxon signed rank test, Fisher's variance test, and Shapiro-Wilks test of the normality of the final model were all greater than 0.398.

Moreover, the influence of the protein-binding parameter, E_{max}, on the CL/*F* estimates for a given patient (5 years old and 20 kg BW) at various doses (5–60 mg/kg) was investigated. The CL/*F* values derived from the DDE model by changing the E_{max} coefficient from 0.5 to 4 (increasing CL/*F* from 1.5- to 5-fold) were compared with those derived from the simple power exponent model. Figure 4 shows that when the TDD was not included in the model, the CL/*F* did not change with the applied dose. However, increased CL/*F* was observed in both the DDE model and the simple exponent model in a dose-dependent manner. The simple exponent model had a higher CL/*F* than the DDE model, in which E_{max} ranged from 0.5 to 2.8, especially at high doses (45–60 mg/kg). Moreover, if E_{max} increased to 4, the CL/*F* versus TDD curves largely overlapped when using the simple exponent model.

Furthermore, decreasing or increasing the k_a by fourfold for each formulation in the final model did not change the final estimates by 9.0 %, except that of the V_d/F (11.7 %), which was consistent with a previous study showing that the k_a had no obvious impact on CL/*F* estimates [45].

3.4 Simulation of Dosing Regimens

The predicted VPA TDD at given trough concentrations of 50 mg/L in children are presented in Fig. 5. The TDD per weight to maintain a given trough concentration increased

Table 3 A summary of external evaluation

Candidate models	Shenyang Shengjing Hospital 82 patients with 137 VPA measurements				Beijing Tian Tan Hospital 50 patients with 147 VPA measurements			
	MPE (%)	MAE (%)	80 %[a]	70 %[b]	MPE (%)	MAE (%)	80 %[a]	70 %[b]
Base model	−0.2 ± 80.8	47.8 ± 65.0	28.5	46.0	9.7 ± 54.5	42.1 ± 35.8	25.9	41.5
Linear pharmacokinetic model[c]	−5.8 ± 58.3	38.2 ± 44.3	34.3	51.1	20.6 ± 54.2	42.2 ± 39.7	27.2	49.6
Simple exponent model (model VII)	11.3 ± 63.4	35.6 ± 53.6	41.6	66.4	5.7 ± 39.2	27.8 ± 28.1	46.2	68.7
Dose-dependent E_{max} model (model VIII)	10.6 ± 61.0	34.8 ± 51.2	43.1	67.2	6.0 ± 39.5	27.4 ± 28.6	46.2	66.7
Protein-binding model (model IX)	6.0 ± 62.2	35.8 ± 51.1	40.9	64.2	10.7 ± 42.3	29.5 ± 32.1	44.2	66.7

Data are expressed as mean ± standard deviation

E_{max} maximum effect, *MAE* mean absolute prediction error, *MPE* mean prediction error, *VPA* valproic acid

[a] The percentage of population prediction error within ±20 %

[b] The percentage of population prediction error within ±30 %

[c] The linear pharmacokinetic model represented the proposed final model without the dose component

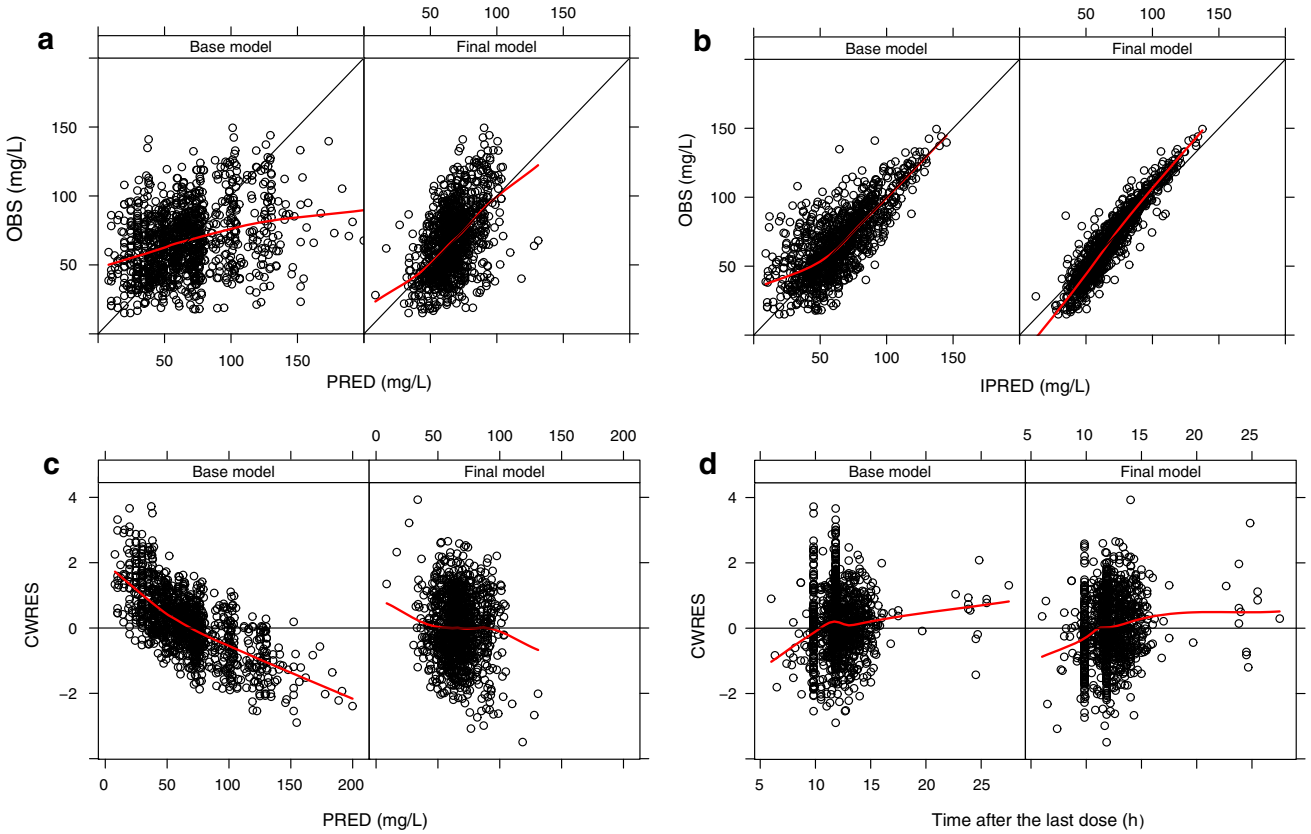

Fig. 2 Goodness-of-fit plot for the base model and the final model. **a** The OBS versus PRED, **b** the OBS versus the Bayesian IPRED, **c** the CWRES versus PRED, **d** the CWRES versus time after the last dose. *Solid lines* in **a** and **b** represent lines of identity. *Red lines* represent LOESS smoothing. *CWRES* conditional weighted residuals, *IPRED* individual predicted concentrations, *OBS* observed concentrations, *PRED* population predicted concentrations

from 6 months, peaked at 1.0 years, and then declined thereafter. For example, maintenance monotherapy of 14 mg/kg in a 8.4-kg child (aged 6 months), 20 mg/kg in a 10-kg child (aged 1 year), and 15 mg/kg in a 15-kg child (aged 4 years) administered twice daily at 12-h intervals can achieve the VPA target concentration of 50 mg/L.

4 Discussion

This is the largest population pharmacokinetic study of VPA conducted to date in pediatric epilepsy patients, and it covers a large age range, from 3 weeks to 14 years. In this study, we first proposed using a DDE model to describe the

Table 4 A summary of the parameters of the valproic acid population model using 2,000 bootstrap runs and NONMEM® estimation

Parameters	NONMEM®		Bootstrap[a]		Bias[b] (%)
	Estimate (% SE)	95 % confidence interval	Estimate	2.5th–97.5th percentiles	
CL_p (L/h)	0.300 (7.9)	0.254–0.346	0.301	0.252–0.361	0.3
Effect of co-medication of carbamazepine on CL/*F*	1.43 (2.7)	1.35–1.51	1.43	1.35–1.51	0
Age-dependent exponent model (model VI)					
k_0	0.791 (2.2)	0.757–0.825	0.791	0.746–0.830	0
k_{max}	0.096 (16.8)	0.065–0.128	0.098	0.063–0.134	2.1
k_{50} (years)	0.802 (11.3)	0.624–0.980	0.802	0.606–1.104	0
Hill coefficient (γ_1)	8.63[c]	–	8.63[c]	–	–
Dose-dependent E_{max} model (model VIII)					
TDD_{50} (mg/kg)	37.4 (15.1)	26.3–48.5	37.5	26.9–53.5	0.3
Hill coefficient (γ_2)	1.68 (6.1)	1.48–1.88	1.70	1.44–2.01	1.2
E_{max}	2.8 fixed	–	2.8 fixed	–	–
V_p·(BW/70) (L/70 kg)	22.2 (8.6)	18.4–26.0	22.2	15.2–37.0	0
$\omega_{CL/F}$	0.195 (9.4)	0.159–0.231	0.195	0.171–0.221	0
η-shrinkage (%)	21.8	–	–	–	–
σ (additive, mg/L)	13.3 (8.4)	10.9–15.3	13.2	11.8–14.7	−0.8
ε-shrinkage (%)	29.5	–	–	–	–

BW body weight, *CL/F* apparent total clearance, CL_p typical value of apparent clearance, E_{max} maximum effect, k_0 value of the exponent at a theoretical BW of 0 kg or age at birth, k_{50} the BW or age at which there is a 50 % decrease in the k_{max}, k_{max} maximum decrease, *SE* standard error, V_p typical value of apparent volume of distribution, TDD_{50} total daily dose when E_{max} is increased by 50 %, $\omega CL/F$ inter-subject variability of apparent clearence, σ residual variability

[a] 1,926 of 2,000 bootstrap runs were successful and were used to calculate the point estimates and 2.5th–97.5th percentiles

[b] Bias % = $(\text{Estimate}_{\text{Bootstrap}} - \text{Estimate}_{\text{NONMEM}})/\text{Estimate}_{\text{NONMEM}} \times 100$ %

[c] Because % SE of the Hill coefficient of the age-dependent exponent model was large, this parameter was fixed in the final model

non-linear pharmacokinetic characteristics of VPA in terms of protein-binding saturation. Moreover, a new ADE model was proposed to scale clearance by simultaneously considering both age and BW in pediatric patients. The established model was evaluated using two external study datasets and showed good predictive performance, indicating that this model might facilitate the development of an optimal dosing regimen in children.

Dose is not recommended for inclusion in models used in population pharmacokinetic analyses, based on sparse samples in TDM settings, due to the TDM effect [20]. The inherent correlation of clearance and dose could be confounded with true non-linearities owing to concentration-dependent protein binding of VPA [11].

The simple exponent model was not appropriate to describe the non-linear pharmacokinetic profiles due to the confounded TDM effect. Therefore, we proposed the DDE model to characterize the non-linear pharmacokinetic of VPA by introducing the parameter of E_{max}; the observed nonlinearity might reflect the change of f_u with dose because this pharmacokinetic component described the non-linear profile of the CL/*F*. Another candidate model, the protein-binding model (model IX), simultaneously reflected the non-linear profiles of CL/*F* and V_d/F. However, this model did not provide better predictive performance that could be attributed to the difference of protein-binding parameters of K_d and B_m, between these two study cohorts. According to the AIC and BIC values as well as the predictive performance of the two models, the DDE model best fitted the aim of the study, although there were no obvious differences in the predictive performances.

In the current study, the simple exponent model indicated that there was a combined non-linear effect of TDM and protein-binding saturation, and a difference in the CL/*F* between the simple exponent and DDE models implies the existence of a TDM effect. Sensitivity analysis of E_{max}, as shown in Fig. 4, indicated that the TDM effect was associated with the degree of non-linearity and that the TDM effect decreased as the non-linear parameter E_{max} increased. The proposed model ($E_{max} = 2.8$) indicated that the TDM effect was increased by dose, and this was obvious when the dose was >50 mg/kg. Individuals being administered more than one dose level was recommended to determine non-linearity and avoid the TDM effect. In our study, the estimated value of E_{max} of 3.05 based on 92 patients at more than one dose level was slightly higher

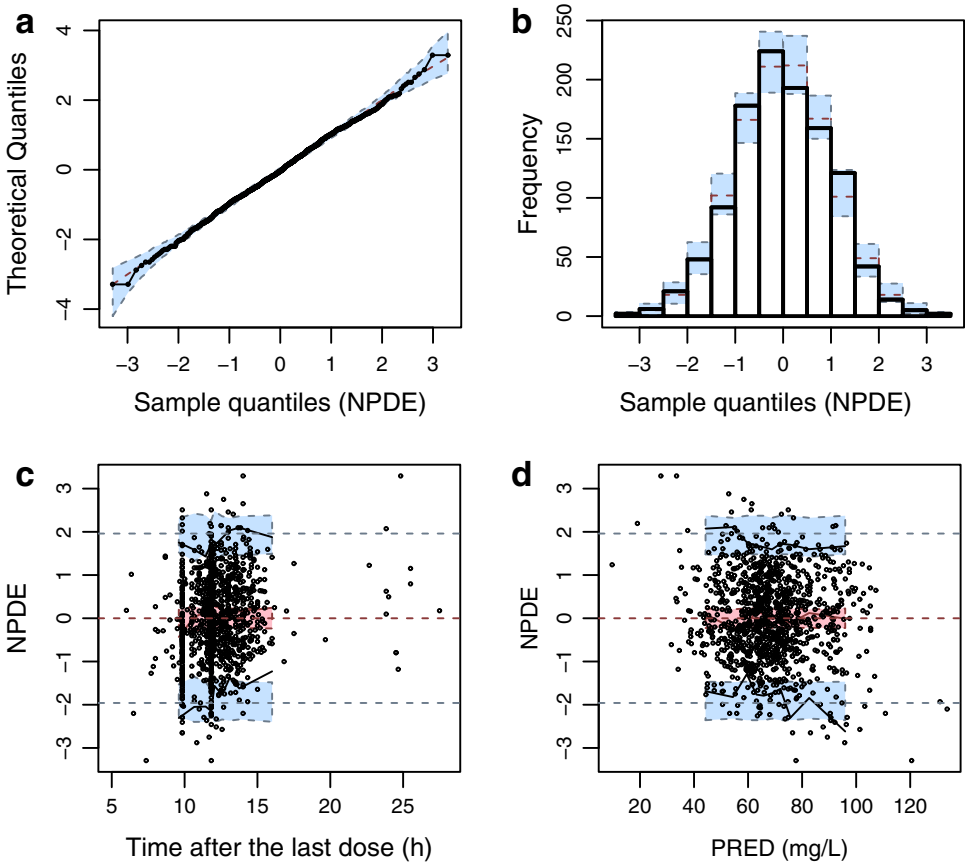

Fig. 3 NPDE of the final population pharmacokinetics model. **a** *Q–Q* plot of the NPDE, **b** histogram of the NPDE, **c** NPDE versus time after the last dose, **d** NPDE versus PRED. *NPDE* normalized prediction distribution errors, *PRED* population predicted concentration

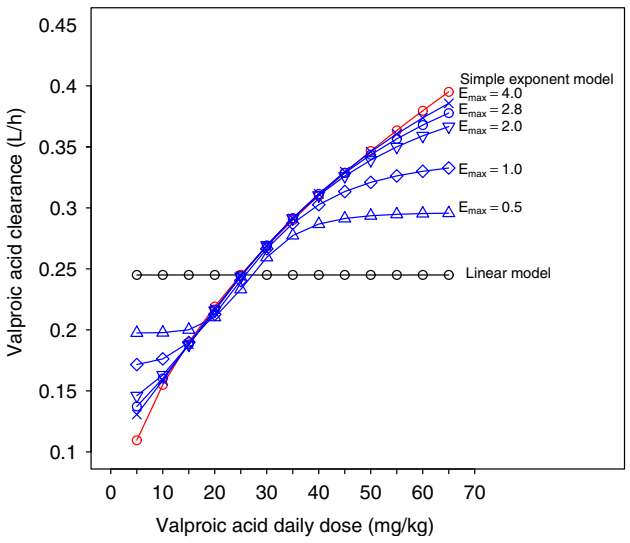

Fig. 4 A comparison of the linear pharmacokinetic model, simple exponent model, and various DDE models with different exponents. The CL/*F* values are derived from the DDE model by changing the E_{max} coefficient from 0.5 to 4 (increasing CL/*F* from 1.5- to 5-fold). *CL/F* apparent total clearance, *DDE* dose-dependent E_{max}, E_{max} maximum effect

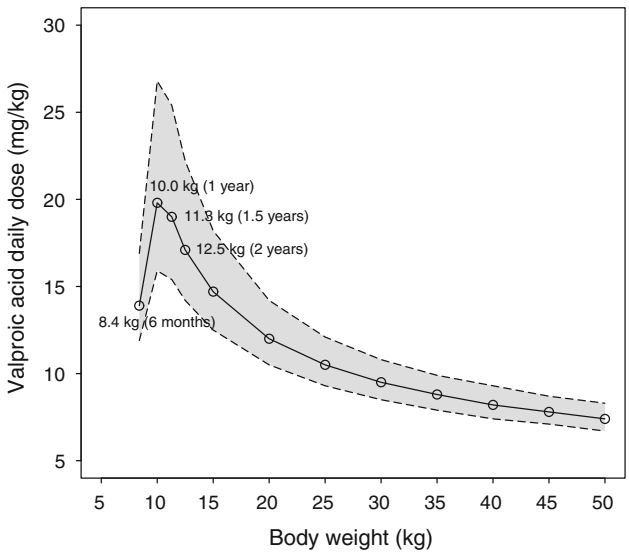

Fig. 5 Predicted valproic acid daily dose at target steady-state trough concentrations of 50 mg/L in pediatric patients with epilepsy using the final model The *shaded areas* represent the 2.5th–97.5th percentiles of the predicted daily dose. The *solid line* represents the median of the predicted daily dose

than that obtained using the final model; this result supports the validity of fixing E_{max} at 2.8.

BW is well-known to be an important covariate in dosing regimens for pediatric patients. The 3/4 allometric scaling approach has been widely used to scale clearance [24, 46, 47]. However, the value of the allometric exponent of 0.75 is debated because this value might be insufficient to describe clearance in infants, toddlers, and young children [26, 27, 48]. This approach has been reported to over-predict clearances for neonates and to under-predict clearance for infants [27]. In contrast, the BDE model scales clearance over the entire human lifespan well; thus, the BDE model is superior to the age-cutoff model and the 0.75 allometric exponent model [29, 49]. However, the age factor, which is naturally related to development, is not considered in the BDE model. Our study developed an ADE model to scale the clearance; this model considers both age and BW, resulting in better model fit than the BDE model.

Interestingly, according to our model, the exponent of BW decreased rapidly from 3 weeks to 1.0 years and was stable after 2.0 years; thus, the model can be simplified to a simple exponent model based on BW for children older than 2.0 years. This finding implies that both age and BW determine maturation simultaneously in children younger than 2.0 years, whereas BW is the most important factor in children older than 2.0 years. These early age-dependent pharmacokinetics may partially reflect the maturation of uridine diphosphate glucuronosyltransferase (UGT) 1A9 and UGT1A6, enzymes that mediate VPA elimination in the liver; these enzymes reach adult levels at 2 years [50] and 14 months [51], respectively. Meanwhile, the expression of another UGT enzyme (UGT2B7), which is also involved in VPA elimination [52], reaches adult levels between 2 and 6 months [53], which is consistent with the rapidly decreasing exponent observed in the ADE model.

Enzyme inducers can increase the CL/*F* of VPA in both children and adults [16, 18, 21, 44]. In the current study, carbamazepine was identified as an important covariate and it increases VPA CL/*F* by approximately 43 %; this value is consistent with that found in previous studies (36–41 %) [18, 21, 54]. Moreover, our study showed that neither co-medicated with clonazepam and topiramate nor sex were covariates, which is also consistent with previous reports [14, 16].

The free concentration of VPA can provide additional information on the non-linearity due to protein-binding saturation. However, this measure is not commonly determined in routine TDM; thus, the proposed model based on the total concentration may not fully reflect the non-linear pharmacokinetic profile of VPA. Moreover, high-dose VPA therapy may impair the β-oxidation route [55], resulting in a non-linearly decreased clearance. This hypothesis requires further investigation.

5 Conclusion

The proposed DDE model successfully described the non-linear pharmacokinetics of VPA based on protein-binding saturation. Furthermore, the final population pharmacokinetic model predicts the individual clearance of a given pediatric patient administered with VPA monotherapy or concomitant carbamazepine in terms of BW and age and can provide a rational dosage recommendation for maintaining concentrations within the desired range.

Acknowledgments This work was partially presented at the 2013 International Symposium of Quantitative Pharmacology, Beijing, China. The authors would like to thank Professor Nick Holford of the University of Auckland, New Zealand for his invaluable advice.

This project was partly supported by the National Natural Science Foundation of China (No. 81072702) and the Major Research and Development Project of Innovative Drugs, China Ministry of Science and Technology (2012ZX09303004-001).

Conflicts of interest All authors declare no conflicts of interest.

References

1. Mac TL, Tran DS, Quet F, Odermatt P, Preux PM, Tan CT. Epidemiology, aetiology, and clinical management of epilepsy in Asia: a systematic review. Lancet Neurol. 2007;6:533–43.
2. Kwong KL, Tsui KW, Wu SP, Yung A, Yau E, Eva F, et al. Utilization of antiepileptic drugs in Hong Kong children. Pediatr Neurol. 2012;46:281–6.
3. Nicholas JM, Ridsdale L, Richardson MP, Ashworth M, Gulliford MC. Trends in antiepileptic drug utilisation in UK primary care 1993-2008: cohort study using the General Practice Research Database. Seizure. 2012;21:466–70.
4. Alehan FK, Morton LD, Pellock JM. Treatment of absence status with intravenous valproate. Neurology. 1999;52:889–90.
5. Brodie MJ, Dichter MA. Antiepileptic drugs. N Engl J Med. 1996;334:168–75.
6. Ito M, Ikeda Y, Arnez JG, Finocchiaro G, Tanaka K. The enzymatic basis for the metabolism and inhibitory effects of valproic acid: dehydrogenation of valproyl-CoA by 2-methyl-branched-chain acyl-CoA dehydrogenase. Biochim Biophys Acta. 1990;1034:213–8.
7. Argikar UA, Remmel RP. Effect of aging on glucuronidation of valproic acid in human liver microsomes and the role of UDP-glucuronosyltransferase UGT1A4, UGT1A8, and UGT1A10. Drug Metab Dispos. 2009;37:229–36.
8. Tan L, Yu JT, Sun YP, Ou JR, Song JH, Yu Y. The influence of cytochrome oxidase CYP2A6, CYP2B6, and CYP2C9 polymorphisms on the plasma concentrations of valproic acid in epileptic patients. Clin Neurol Neurosurg. 2010;112:320–3.
9. Kodama Y, Koike Y, Kimoto H, Yasunaga F, Takeyama M, Teraoka I, et al. Binding parameters of valproic acid to serum protein in healthy adults at steady state. Ther Drug Monit. 1992;14:55–60.

10. Bauer LA, Davis R, Wilensky A, Raisys V, Levy RH. Valproic acid clearance: unbound fraction and diurnal variation in young and elderly adults. Clin Pharmacol Ther. 1985;37:697–700.
11. Zaccara G, Messori A, Moroni F. Clinical pharmacokinetics of valproic acid. Clin Pharmacokinet. 1988;15:367–89.
12. Patsalos PN, Berry DJ, Bourgeois BF, Cloyd JC, Glauser TA, Johannessen SI, et al. Antiepileptic drugs–best practice guidelines for therapeutic drug monitoring: a position paper by the subcommission on therapeutic drug monitoring, ILAE Commission on Therapeutic Strategies. Epilepsia. 2008;49:1239–76.
13. Williams JH, Jayaraman B, Swoboda KJ, Barrett JS. Population pharmacokinetics of valproic acid in pediatric patients with epilepsy: considerations for dosing spinal muscular atrophy patients. J Clin Pharmacol. 2012;52:1676–88.
14. Jiang DC, Wang L, Wang YQ, Li L, Lu W, Bai XR. Population pharmacokinetics of valproate in Chinese children with epilepsy. Acta Pharmacol Sin. 2007;28:1677–84.
15. Sanchez-Alcaraz A, Quintana MB, Lopez E, Rodriguez I. Valproic acid clearance in children with epilepsy. J Clin Pharm Ther. 1998;23:31–4.
16. Yu L, Ding J, Shi H, Li Z, Jiao Z, Wang Y. Establishment of population pharmacokinetic model of valproic acid in Chinese epileptic children. Chin J Evid Based Pediatr. 2009;6:509–13. [in Chinese]
17. Yukawa E, To H, Ohdo S, Higuchi S, Aoyama T. Population-based investigation of valproic acid relative clearance using nonlinear mixed effects modeling: influence of drug-drug interaction and patient characteristics. J Clin Pharmacol. 1997;37:1160–7.
18. Serrano BB, Garcia SM, Otero MJ, Buelga DS, Serrano J, Dominguez-Gil A. Valproate population pharmacokinetics in children. J Clin Pharm Ther. 1999;24:73–80.
19. Correa T, Rodriguez I, Romano S. Population pharmacokinetics of valproate in Mexican children with epilepsy. Biopharm Drug Dispos. 2008;29:511–20.
20. Ahn JE, Birnbaum AK, Brundage RC. Inherent correlation between dose and clearance in therapeutic drug monitoring settings: possible misinterpretation in population pharmacokinetic analyses. J Pharmacokinet Pharmacodyn. 2005;32:703–18.
21. Jiao Z, Zhong M, Hu M, Shi X, Li Z, Zhang J, et al. Population pharmacokinetic modeling of valproic acid clearance. Chin Hosp Pharm J. 2004;9:515–8 [in Chinese].
22. Bano G, Gupta S, Gupta KL, Raina RK. Pharmacokinetics of valproic acid after administration of three oral formulations in healthy adults. J Assoc Phys India. 1990;38:629–30.
23. Hou Q, Qu Z, Yu L, Zhang J. Comparison of pharmacokinetics, plasma concentration and efficacy between valproic acid sustained released and enteric-coated tablets. Chin J Neurol Psychiatry. 1993;26:165 [in Chinese].
24. Holford N, Heo YA, Anderson B. A pharmacokinetic standard for babies and adults. J Pharm Sci. 2013;102:2941–52.
25. Anderson BJ, McKee AD, Holford NH. Size, myths and the clinical pharmacokinetics of analgesia in paediatric patients. Clin Pharmacokinet. 1997;33:313–27.
26. Mahmood I. Prediction of drug clearance in children from adults: a comparison of several allometric methods. Br J Clin Pharmacol. 2006;61:545–57.
27. Peeters MY, Allegaert K, Blusse VOH, Cella M, Tibboel D, Danhof M, et al. Prediction of propofol clearance in children from an allometric model developed in rats, children and adults versus a 0.75 fixed-exponent allometric model. Clin Pharmacokinet. 2010;49:269–75.
28. Kodama Y, Kodama H, Kuranari M, Tsutsumi K, Ono S, Fujimura A. No effect of gender or age on binding characteristics of valproic acid to serum proteins in pediatric patients with epilepsy. J Clin Pharmacol. 1999;39:1070–6.
29. Wang C, Peeters MY, Allegaert K, Blusse VOH, Krekels EH, Tibboel D, et al. A bodyweight-dependent allometric exponent for scaling clearance across the human life-span. Pharm Res. 2012;29:1570–81.
30. Cloyd JC, Dutta S, Cao G, Walch JK, Collins SD, Granneman GR. Valproate unbound fraction and distribution volume following rapid infusions in patients with epilepsy. Epilepsy Res. 2003;53:19–27.
31. Ueshima S, Aiba T, Makita T, Nishihara S, Kitamura Y, Kurosaki Y, et al. Characterization of non-linear relationship between total and unbound serum concentrations of valproic acid in epileptic children. J Clin Pharm Ther. 2008;33:31–8.
32. Ueshima S, Aiba T, Sato T, Matsunaga H, Kurosaki Y, Ohtsuka Y, et al. Empirical approach for improved estimation of unbound serum concentrations of valproic acid in epileptic infants by considering their physical development. Biol Pharm Bull. 2011;31:108–13.
33. Holford N. Protein binding model. http://www.cognigencorp.com/nonmem/current/2011-May/2497.html. Accessed 15 Jun 2014.
34. Savic RM, Karlsson MO. Importance of shrinkage in empirical bayes estimates for diagnostics: problems and solutions. AAPS J. 2009;11:558–69.
35. Keizer RJ, van Benten M, Beijnen JH, Schellens JH, Huitema AD. Pirana and PCluster: a modeling environment and cluster infrastructure for NONMEM. Comput Methods Progr Biomed. 2011;101:72–9.
36. Byon W, Smith MK, Chan P, Tortorici MA, Riley S, Dai H, et al. Establishing best practices and guidance in population modeling: an experience with an internal population pharmacokinetic analysis guidance. CPT Pharmacometr Syst Pharmacol. 2013;2:e51.
37. Tunblad K, Lindbom L, McFadyen L, Jonsson EN, Marshall S, Karlsson MO. The use of clinical irrelevance criteria in covariate model building with application to dofetilide pharmacokinetic data. J Pharmacokinet Pharmacodyn. 2008;35:503–26.
38. Staatz CE, Duffull SB, Kiberd B, Fraser AD, Tett SE. Population pharmacokinetics of mycophenolic acid during the first week after renal transplantation. Eur J Clin Pharmacol. 2005;61:507–16.
39. Gotta V, Buclin T, Csajka C, Widmer N. Systematic review of population pharmacokinetic analyses of imatinib and relationships with treatment outcomes. Ther Drug Monit. 2013;35:150–67.
40. Guo Y, Hu C, He X, Qiu F, Zhao L. Effects of UGT1A6, UGT2B7, and CYP2C9 genotypes on plasma concentrations of valproic acid in Chinese children with epilepsy. Drug Metab Pharmacokinet. 2012;27:536–42.
41. van der Meer AF, Marcus MA, Touw DJ, Proost JH, Neef C. Optimal sampling strategy development methodology using maximum a posteriori Bayesian estimation. Ther Drug Monit. 2011;33:133–46.
42. Ette EI, Williams PJ, Kim YH, Lane JR, Liu MJ, Capparelli EV. Model appropriateness and population pharmacokinetic modeling. J Clin Pharmacol. 2003;43:610–23.
43. Comets E, Brendel K, Mentre F. Computing normalised prediction distribution errors to evaluate nonlinear mixed-effect models: the npde add-on package for R. Comput Methods Programs Biomed. 2008;90:154–66.
44. Li H, Ji CY, Zong XN, Zhang YQ. Height and weight standardized growth charts for Chinese children and adolescents aged 0 to 18 years [in Chinese]. Chin J Pediatr. 2009;47:487–92.
45. Wade JR, Kelman AW, Howie CA, Whiting B. Effect of misspecification of the absorption process on subsequent parameter estimation in population analysis. J Pharmacokinet Biopharm. 1993;21:209–22.

46. Anand KJ, Anderson BJ, Holford NH, Hall RW, Young T, Shephard B, et al. Morphine pharmacokinetics and pharmacodynamics in preterm and term neonates: secondary results from the NEOPAIN trial. Br J Anaesth. 2008;101:680–9.
47. Anderson BJ, Allegaert K, Van den Anker JN, Cossey V, Holford NH. Vancomycin pharmacokinetics in preterm neonates and the prediction of adult clearance. Br J Clin Pharmacol. 2007;63:75–84.
48. Bjorkman S. Prediction of cytochrome p450-mediated hepatic drug clearance in neonates, infants and children: how accurate are available scaling methods? Clin Pharmacokinet. 2006;45:1–11.
49. Bartelink IH, Boelens JJ, Bredius RG, Egberts AC, Wang C, Bierings MB, et al. Body weight-dependent pharmacokinetics of busulfan in paediatric haematopoietic stem cell transplantation patients: towards individualized dosing. Clin Pharmacokinet. 2012;51:331–45.
50. Choonara IA, McKay P, Hain R, Rane A. Morphine metabolism in children. Br J Clin Pharmacol. 1989;28:599–604.
51. Miyagi SJ, Collier AC. The development of UDP-glucuronosyltransferases 1A1 and 1A6 in the pediatric liver. Drug Metab Dispos. 2011;39:912–9.
52. Ethell BT, Anderson GD, Burchell B. The effect of valproic acid on drug and steroid glucuronidation by expressed human UDP-glucuronosyltransferases. Biochem Pharmacol. 2003;65:1441–9.
53. Ebner T, Burchell B. Substrate specificities of two stably expressed human liver UDP-glucuronosyltransferases of the UGT1 gene family. Drug Metab Dispos. 1993;21:50–5.
54. Blanco-Serrano B, Otero MJ, Santos-Buelga D, Garcia-Sanchez MJ, Serrano J, Dominguez-Gil A. Population estimation of valproic acid clearance in adult patients using routine clinical pharmacokinetic data. Biopharm Drug Dispos. 1999;20:233–40.
55. Lheureux PE, Hantson P. Carnitine in the treatment of valproic acid-induced toxicity. Clin Toxicol (Phila). 2009;47:101–11.